

The Interrelated Pollution Characteristics of Atmospheric Speciated Mercury and Water-Soluble Inorganic Ions in Ningbo, China

Hui Yi ^{1,2,3,†}, Dan Li ^{1,2,3,†}, Jianrong Li ^{1,3}, Lingling Xu ¹, Zhongwen Huang ⁴, Hang Xiao ^{1,3,*} and Lei Tong ^{1,3,*}

¹ Center for Excellence in Regional Atmospheric Environment & Fujian Key Laboratory of Atmospheric Ozone Pollution Prevention & Key Laboratory of Urban Environment and Health, Institute of Urban Environment, Chinese Academy of Sciences, Xiamen 361021, China; hyi@iue.ac.cn (H.Y.); dli@iue.ac.cn (D.L.); jrli@iue.ac.cn (J.L.); linglingxu@iue.ac.cn (L.X.)

² University of Chinese Academy of Sciences, Beijing 100049, China

³ Zhejiang Key Laboratory of Urban Environmental Process and Pollution Control, Ningbo (Beilun) Zhongke Haixi Industrial Technology Innovation Center, Ningbo 315800, China

⁴ School of Chemistry and Environmental Engineering, Hanzhou Normal University, Chaozhou 521000, China; huangzw@hstc.edu.cn

* Correspondence: hxiao@iue.ac.cn (H.X.); ltong@iue.ac.cn (L.T.); Tel.: +86-574-8678-4813 (H.X.); Fax: +86-574-8678-4813 (H.X.)

† These two authors have contributed equally to this paper.

Abbreviations Index

Danish Eulerian Hemispheric Model (DEHM)
Global/Regional Atmospheric Heavy Metals Model (GRAHM)
Global EMEP Multi-media Modelling System (GLEMOS)
Global EMEP Multi-media Modelling System (GEOS-Chem)
Gas-particle partitioning coefficients (K_p)
gaseous elemental mercury (GEM)
gaseous oxidized mercury (GOM)
mean absolute percent error (MAE)
maximum absolute percent error (MAPE)
Ningbo urban environment observation and research station (NUEORS)
potential source contribution function (PSCF)
particle bound mercury (PBM)
root mean square error (RMSE)
sulfate, nitrate and ammonium (SNA)
total water-soluble inorganic ions (TWSI)
total gaseous mercury concentrations (TGM)
temperature (T)
water-soluble inorganic ions (WSIIs)
Yangtze river delta (YRD)

Caption for All the Figures/Tables

Figure S1. Schematic of the Piper diagram (The red point in the bottom-left panel indicates the percentage values of cations, which were 40%, 40% and 20% for $[\text{Na}^+ + \text{Mg}^{2+}]$, $[\text{K}^+ + \text{Ca}^{2+}]$ and $[\text{NH}_4^+]$, respectively. The red point in the bottom-right panel indicates the percentage values of anions, which were 60%, 20% and 20% for Cl^- , SO_4^{2-} and NO_3^- , respectively. As to the top panel, the four dimensions ($[\text{SO}_4^{2-}]$, $[\text{NH}_4^+]$, $[\text{Cl}^- + \text{NO}_3^-]$ and $[\text{Na}^+ + \text{Mg}^{2+} + \text{K}^+ + \text{Ca}^{2+}]$) of the red point were 20%, 20%, 80% and 80%, respectively. The Piper diagram for aerosol research could be used to reflect the potential sources for atmospheric mercury.)

Figure S2. The relationship between GOM and WSIIs

Figure S3. 72-h backward trajectories during the pollution episode ((a) and (b): from 00:00 on October 21 to 23:00 on October 22, (c) and (d): from 00:00 on October 23 to 23:00 on October 24. The backward trajectories were generated with 1h time resolution.)

Table S1. Summary of GEM, GOM, PBM, $\text{PM}_{2.5}$ and WSIIs concentrations

Table S2. The Spearman correlation of speciated mercury with WSIIs and conventional pollutants during the pollution episode from October 21 to October 24, 2017

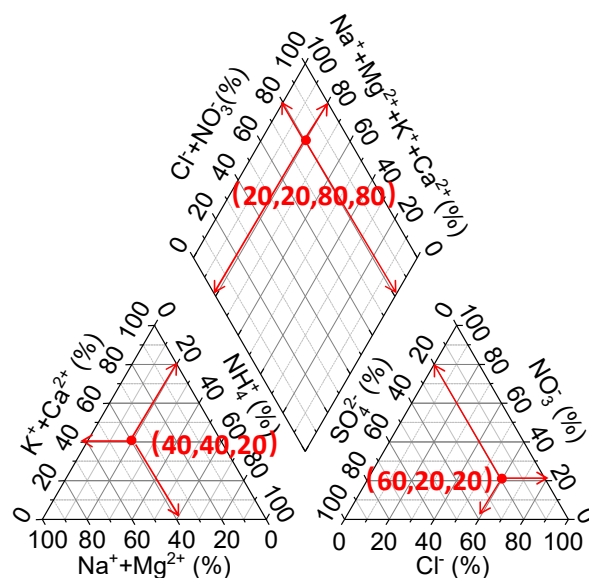


Figure S1. Schematic of the Piper diagram (The red point in the bottom-left panel indicates the percentage values of cations, which were 40%, 40% and 20% for $[\text{Na}^+ + \text{Mg}^{2+}]$, $[\text{K}^+ + \text{Ca}^{2+}]$ and $[\text{NH}_4^+]$, respectively. The red point in the bottom-right panel indicates the percentage values of anions, which were 60%, 20% and 20% for Cl^- , SO_4^{2-} and NO_3^- , respectively. As to the top panel, the four dimensions ($[\text{SO}_4^{2-}]$, $[\text{NH}_4^+]$, $[\text{Cl}^- + \text{NO}_3^-]$ and $[\text{Na}^+ + \text{Mg}^{2+} + \text{K}^+ + \text{Ca}^{2+}]$) of the red point were 20%, 20%, 80% and 80%, respectively. The Piper diagram for aerosol research could be used to reflect the potential sources for atmospheric mercury.)

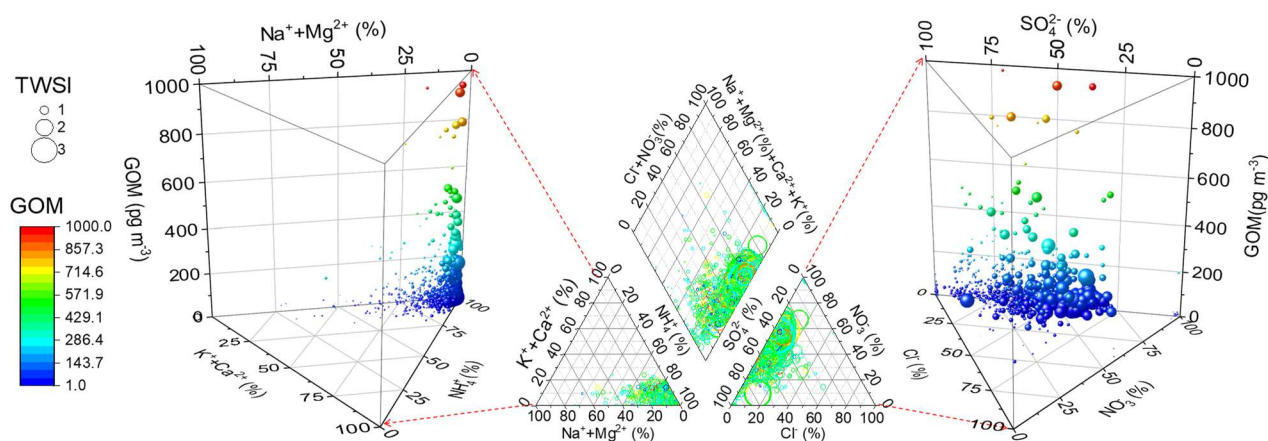


Figure S2. The relationship between GOM and WSIs

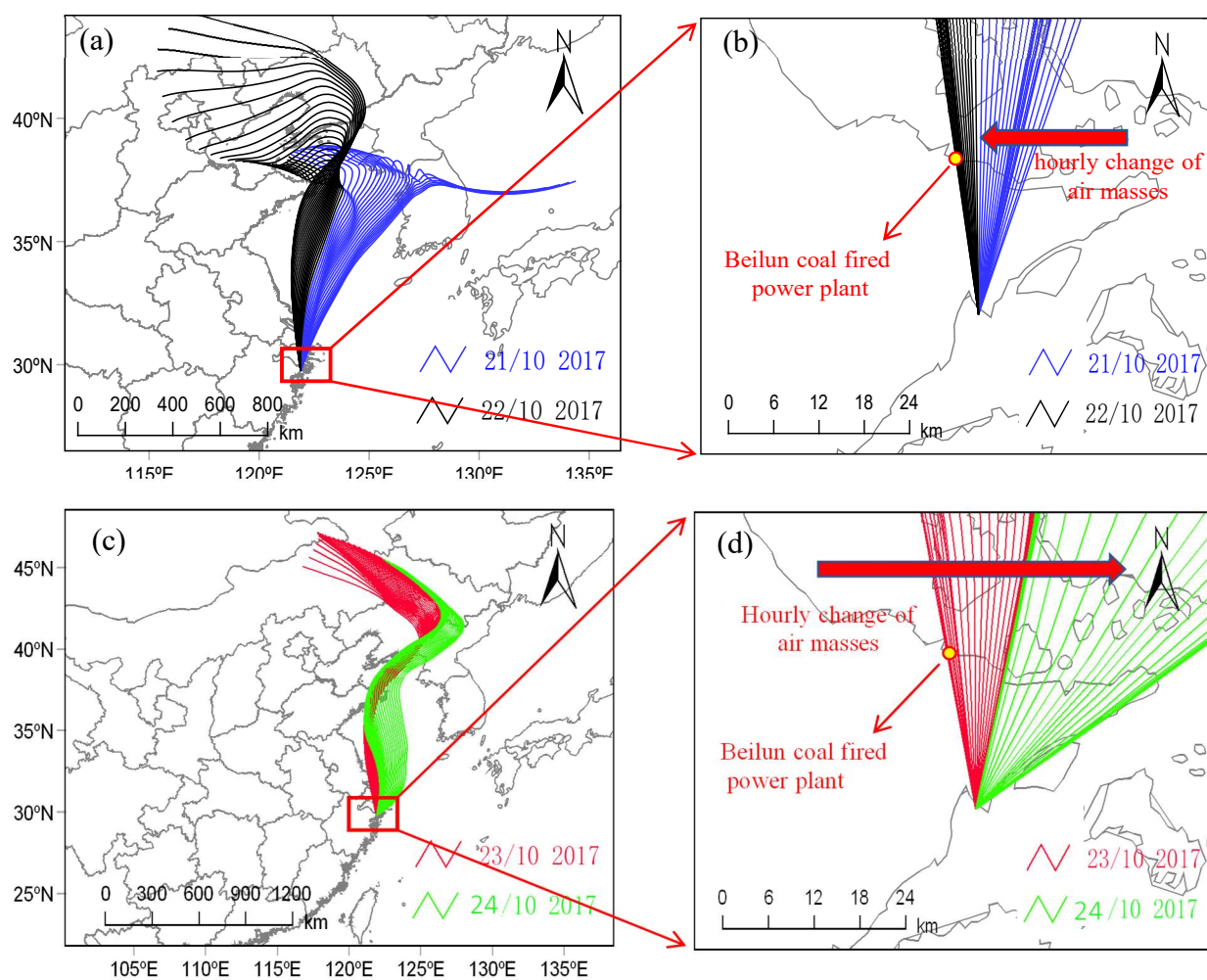


Figure S3. 72-h backward trajectories during the pollution episode ((a) and (b): from 00:00 on October 21 to 23:00 on October 22, (c) and (d): from 00:00 on October 23 to 23:00 on October 24. The backward trajectories were generated with 1h time resolution.)

Table S1. Summary of GEM, GOM, PBM, PM_{2.5} and WSII_s concentrations

	Mean	Median	SD	Min.	Max.	Percentiles		
						25	50	75
GEM (ng m ⁻³)	2.4	2.2	0.9	0.6	10.9	1.8	2.2	2.8
GOM (pg m ⁻³)	99.3	43.5	199.5	1.7	2591.4	21.3	43.5	97.1
PBM (pg m ⁻³)	286.5	132.5	448.0	1.6	5372.5	50.8	132.5	335.0
PM _{2.5} (µg m ⁻³)	25.1	20.6	17.2	0.1	130.0	13.1	20.6	32.2
Cl ⁻ (µg m ⁻³)	0.7	0.3	1.0	0.1	9.4	0.1	0.3	1.0
NO ₃ ⁻ (µg m ⁻³)	6.3	3.0	8.1	0.1	66.4	1.4	3.0	7.8
SO ₄ ²⁻ (µg m ⁻³)	7.6	6.4	5.1	0.1	34.3	4.1	6.4	9.9
Na ⁺ (µg m ⁻³)	0.4	0.3	0.3	<DL	3.2	0.2	0.3	0.4
NH ₄ ⁺ (µg m ⁻³)	4.2	2.9	4.0	<DL	28.9	1.5	2.9	5.1
K ⁺ (µg m ⁻³)	0.4	0.3	0.3	<DL	2.7	0.2	0.3	0.4
Mg ²⁺ (µg m ⁻³)	0.1	0.1	0.1	0.1	0.6	0.1	0.1	0.1
Ca ²⁺ (µg m ⁻³)	0.2	0.2	0.1	0.2	1.4	0.1	0.2	0.3

DL: detection limit.

Table S2. The Spearman correlation of speciated mercury with *WSIIs* and conventional pollutants during the pollution episode from October 21 to October 24, 2017

	PM _{2.5}	SO ₄ ²⁻	NO ₃ ⁻	NH ₄ ⁺	K ⁺	Cl ⁻	Na ⁺	Mg ²⁺	Ca ²⁺	SO ₂	NO ₂	CO	O ₃	GEM	GOM	PBM
GEM	0.73**	0.53**	0.74**	0.72**	0.35**	0.69**	-0.35	-0.18	0.19	0.52**	0.49**	0.66**	0.14	1.00	-0.06	0.65**
GOM	-0.01	0.15	-0.10	0.03	-0.26	-0.27	-0.24	-0.22	-0.08	-0.12	-0.24	0.16	0.31*	0.01	1.00	-0.01
PBM	0.54**	0.19	0.67**	0.42**	0.56**	0.55**	-0.07	-0.17	0.36**	0.65**	0.72**	0.27*	-0.20	0.63**	-0.01	1.00

Note: *: $p < 0.05$; **: $p < 0.01$.